2nd International Symposium on Magnetic Beaing
July 12-14, 1990, Tokyo, Japan

AN APPLICATION OF MAGNETIC BEARINGS TO TITANIUM POWDER PRODUCTION

T. KIMURA and T. NEGISHI

Mitsubishi Metal Corp. Central Research Institute
1-297 Kitabukuro, Omiya, Saitama 330, Japan

Abstract

Plasma rotary electrode process (PREP) is being used for production of titanium alloy powder. In this technique, titanium billet is rotated and one end of the billet is melted by plasma arc, and droplets are sprayed by centrifugal force and cooled in an inert atmosphere. The rotating mechanism is like a cantilever arm with a heavy weight top and the critical speed is lowered by the weight of the top. Also there are many vibration sources in this system. To avoid this vibrational problem, we adopted the magnetic bearing as the drive mechanism in place of the motor and gear train. The use of the magnetic bearing resulted in an increase of allowable unbalance and a large decrease of the vibration of the machine. These improvements made it possible to produce fine and rapidly solidified particles with a higher productivity.

1. Introduction

Titanium alloys are very attractive as structural materials because of their superior strength to density ratio, fatigue strength and fracture toughness, but they have two problems, i.e., low production yield and high cost. Powder metallurgy route is considered to be very promising to solve these problems and a substantial amount of work has been carried out[1].

Ti alloys are in general hard to work with, but they show enormous elongation up to 1000% and very low flow stress at some strain rate and temperature condition (Superplasticity) [2]. Therefore, National Research Institute for Metals (NRIM) has developed the designing principle and designed new alloy GT-33(Ti-6.5Al-1.4V-1.4Sn-1.0Zr-2.9Mo-2.1Cr-1.7Fe) which has good superplasticity at working temperature and superior mechanical properties at service temperature[3]. We have developed powder production technology to obtain fine particles of this alloys and superplastic forging technology to obtain complex shaped forgings. In this paper, we report the development of powder production technology and application of magnetic bearings in a PREP chamber.

2. Titanium Powder Production Technology

2.1 Outlook

Titanium alloys are chemically active and react with refractory materials, and ordinary powder production technics such as gas atomizing can not be used. Therefore, rotating electrode process (REP) and plasma rotating electrode process (PREP) are developed by Nuclear Metals Inc. and being used for production of titanium alloy powders[4]. In these techniques as shown in **Fig.1**, titanium billet is rotated and one end of billet is melted by arc or plasma arc, and droplets are sprayed by centrifugal force and cooled in an inert atmosphere. Gas atomizing of titanium alloys using skull melting[5] and centrifugal atomization by rotating disk[6] are attractive alternative technologies to REP. But they are still in development stage.

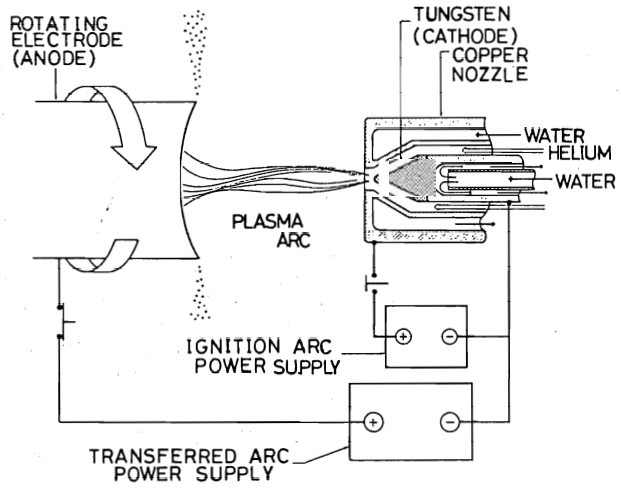

Fig.1 Principle of the transferred arc plasma REP (PREP)[2].

2.2 Particle diameter

In rotating electrode process, molten metal on the top of billet is formed as liquid torus. When the centrifugal force acting on the growing liquid mass overcomes the retaining force of surface tension, liquid protuberances form and drops are ejected from the billet. Considering the balance between these forces, a simple equation is obtained :

$$d=\frac{A}{\omega}\left(\frac{\gamma}{D\rho}\right)^{\frac{1}{2}} \tag{1}$$

d : diameter of particle, μm
ω : angular velocity, rad/s
γ : surface tension of liquid metal, N/m
ρ : density of liquid metal, kg/m^3
D : diameter of billet, m
A : constant

Many authors give the value for constant A and 3.8×10^6 is given for organic liquids[7].

From the regression analysis of many metal atomization experiments, the relation between the mean volume-surface diameter (Sauter diameter) d_{vs} and experimental variables is obtained[8] :

$$d_{vs}=4.63\times10^6\frac{1}{\omega^{0.98}}\frac{1}{D^{0.64}}\left(\frac{\gamma}{\rho}\right)^{0.43}Q^{0.12} \tag{2}$$

Q : melting or flow rate, m^3/s

From these equations, relation between the major parameters are plotted in Fig.2.

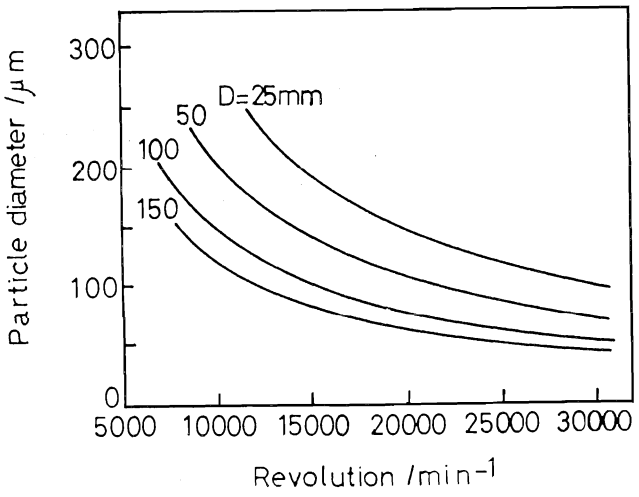

Fig.2 Relation between billet diameter, revolution and particle diameter.

2.3 Cooling rate

A molten droplet is cooled in flight to reflector walls. The mechanisms of heat transfer are radiation and forced convection. The cooling rate of droplets $\dot{T}$(K/s) is given as follows[9] :

$$\dot{T}=\frac{6}{D\rho C_p}\left[h_c\left(T_s-T_g\right)+\sigma\varepsilon\left(T_s^4-T_g^4\right)\right] \tag{3}$$

C_p : specific heat
T_g : temperature of circumferential media
T_s : temperature of droplet
h_c : thermal conductivity
σ : Stephan-Boltzmann constant
ε : emissivity

here h_c is given by

$$h_c=\frac{Nu\cdot\lambda}{d} \tag{4}$$

Nu : Nusselt Number given by

$$Nu=2+0.552Pr^{\frac{1}{3}}Re^{\frac{1}{2}} \tag{5}$$

Pr : Prandtl Number
Re : Reynolds Number

In Eq.3, heat loss by radiation is about several percent of the total heat loss and effect of latent heat is also small.

From the metallurgical point, the relation between cooling (solidification) rate and the secondary dendrite arm spacing (DAS:μm) was studied for Fe, Al, Ni, Cu alloys and formulated as below[10] :

$$\dot{T}=10^5\times\left(DAS\right)^{-3} \tag{6}$$

In Ti alloys, droplet is solidified to the β single phase structure and then decomposes to the $\alpha+\beta$ dual phase structure. The relation between the β grain size $L(\mu m)$ and $\dot{T}$ is given in reference [11] :

$$L=3\times10^6\dot{T}^{-0.9} \tag{7}$$

During the flight, the velocity of droplets is reduced by frictional force and cooling rate is also reduced.

3. Atomizer

3.1 Heat Source and cooling system

Based on the above mentioned formulae, we designed the powder production equipment[12]. The machine was built by ULVAC Corp. Photo.1 shows the appearance of the machine. Photo.2 shows the powder producing condition.

The heat source of this equipment is a plasma torch with a hot hollow cathode discharge[13]. A source gas flows into the heated Ta cathode tube and is excited to plasma, and also thermal electron is ejected out. This system uses the middle position of electron beam and plasma arc, and we named this machine as Plasma Beam Rotary Electrode Process (PBREP).

To obtain rapidly solidified powder, it is necessary to increase circumferential pressure. Therefore, operating pressure is increased gradually and He cooling gas is jet-sprayed perpendicularly into the particle flight path.

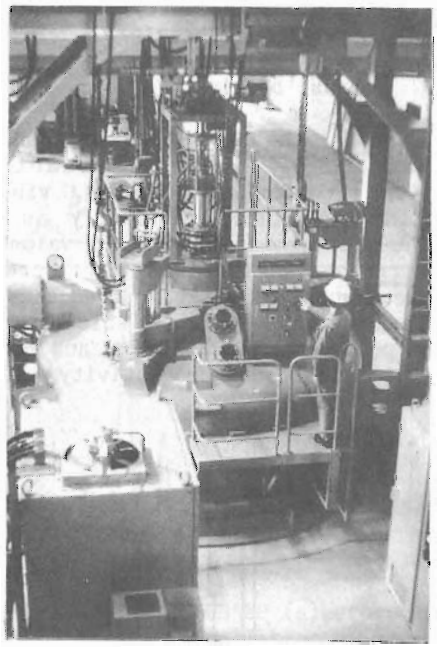

Photo.1 PBREP Machine.

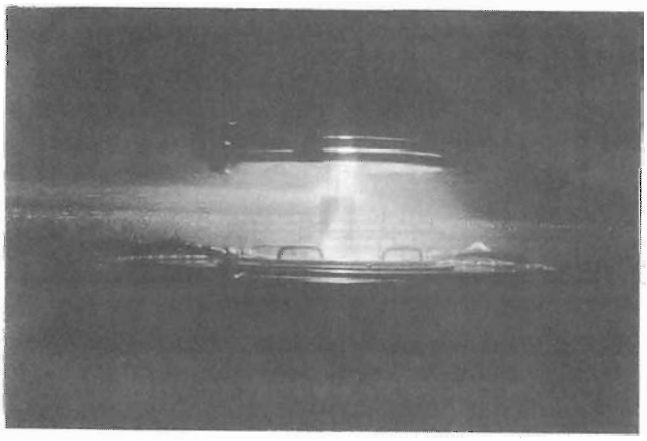

Photo.2 Powder producing condition.

3.2Drive system

To obtain fine and rapidly solidified powder, from Eq.1~7 it is necessary to increase the diameter of billet D and angular velocity ω. These requirements are rather severe for the drive system.

Originally, drive system was made of motor and gear train. Motor and 1st speed increasing gear are in air and transmit to 2nd speed increasing gear in vacuum chamber. As oil with high vapor pressure can not be used in the vacuum, lubrication was not perfect, and high frequency vibration like oil-whip occurred also in gear train.

The output axis fixes the billet. This system is like a cantilever arm with a heavy weight top and the critical speed is lowered by the weight.

When atomizing starts, usually the end of billet is melted nonuniformly and the end portion of the billet heated to just below the melting point deforms by centrifugal force. Consequently the axis starts whirling.

In addition to this, the system is thermally not steady. Heat is conducted from the top end of the billet and is generated in brush assembly by friction, contact resistance and resistivity. As a result, unsymmetrical thermal displacement occurs.

By solving the vibration equation with the boundary conditions of load from the gear and estimated unbalance, maximum operation speed was calculated to be 12,000 RPM.

Then, we redesigned the system to increase the stiffness of axis, and to improve the mounting condition, lubrication, dynamic balance and mechanical tolerances. Further, we avoided the resonance of vibration in each part and installed dynamic damper in the axis. As a result , estimated maximum operation speed is increased to 15,000 RPM. In actual operation, as the atomization proceeds, the vibration amplitude increased and rotation of 4kg billet at 14,000 RPM was the limit.

3.3 Application of magnetic bearing

At that time magnetic bearing was introduced to us by Dr. Harada of NRIM.

The characteristics of magnetic bearing[14] are as follows ;

1. Can be used in vacuum
2. Oil free
3. Increase of natural frequency due to double end free axis
4. Increase of allowable unbalance due to non-contact support
5. Rotation around principal axis of inertia by automatic balancing system

These are very advantageous to the drive system in a vacuum environment.

In this system, motor shaft is levitated by the forces generated by a magnetic field and has 5 degrees of freedom. As shown in **Fig.3**, the position of the shaft is monitored by sensors, signals are feedbacked and active servo system controls the position.

The stiffness of the bearing is given by

$$K=|F/x|=\left\{\left(k_0-M\omega^2\right)^2+\left(a^+\omega-\frac{b}{\omega}\right)^2\right\}^{\frac{1}{2}} \qquad (8)$$

here

M ; weight of rotor
F ; external force
x ; displacement
k_0 ; spring constant
a^+ ; damping factor
b ; constant for integral term

and its relation to frequency is shown in **Fig.4**. Static stiffness is given by b/ω and is relatively large value as compared with that of conventional bearings. Damping factor a^+ of the magnetic bearing is also larger and consequently its dynamic stiffness becomes higher.

Furthermore, this control system has automatic balancing system. In this system, signals from the position sensor passes a narrow band tracking filter and signals of the rotating frequency is ignored. Therefore shaft rotates around its principal axes of inertia[15].

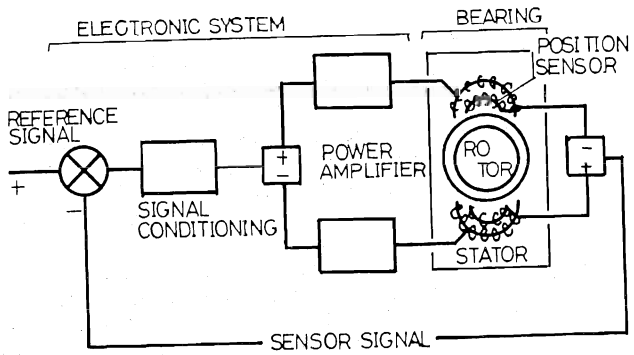

Fig.3 Control loop of magnetic bearings[14].

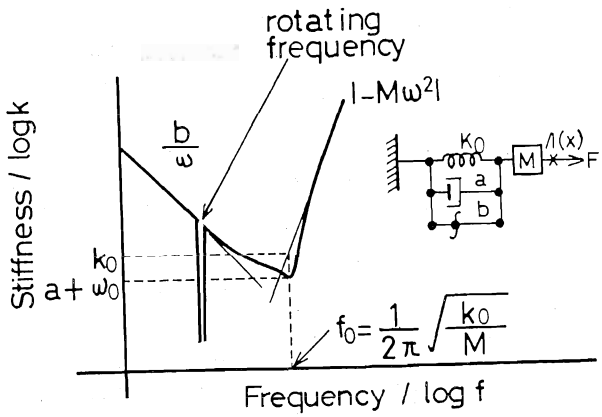

Fig.4 The relation between stiffness and frequency of magnetic bearings[15].

But there was a possibility of mutual electrical interference among electric components in our equipment. The brush assembly was installed just above the end of the motor shaft and transmit DC current up to 2000 A. The brush may cause chattering and arcing. And there existed a magnetic field due to the electric current in the constriction coil of plasma. It was confirmed that there exists no interaction, and we adopted B25/500 magnetic spindle made by S2M as the driving system in place of the motor and the gear train.

Main specification of our magnetic bearings is

Power	15	kw
Maximum rotation speed	24000	RPM
Weight of billet	6	kg
Unbalance	160	gcm max
Maximum load capacity		
upper radial bearing	153	kgf
lower radial bearing	87	kgf
thrust bearing	204	kgf

Fig.5 shows the structure of PBREP after installation of magnetic bearings. By application of magnetic bearings, vibration of the machine decreased drastically as shown in **Fig.6**. The improvement of overall value of power spectrum reached up to 30dB and there is left only the component of rotating frequency.

In operation, we are now able to produce 5 kg/batch powder at 15000 RPM and it may be possible to increase productivity rate using heavier billets.

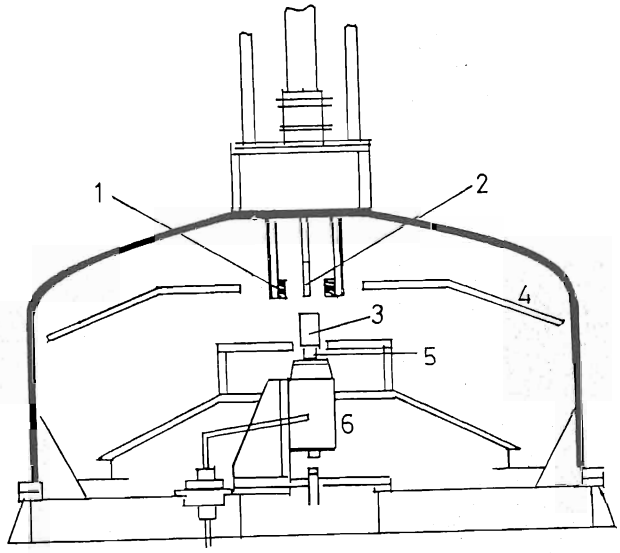

Fig.5 The structure of PBREP after installation of magnetic bearings.
(1) Plasma constriction coil;
(2) plasma torch; (3) billet;
(4) reflector; (5) brush assembly;
(6) magnetic bearings.

As the magnetic bearings give information about the amplitude of vibration and its tendency, the growth rate of unbalance can be calculated. We made several models to explain the phenomena, and now some automatic and manual control are possible. The plasma torch chases the melting billet to keep the distance and is moved to the rim portion of the billet to eliminate the growing unbalance. An example of the change of the vibrational amplitude during atomization is shown in **Fig.7**. Here, only first portion of atomization procedure is shown. The unbalance is improved gradually by the loss of weight of the billet.

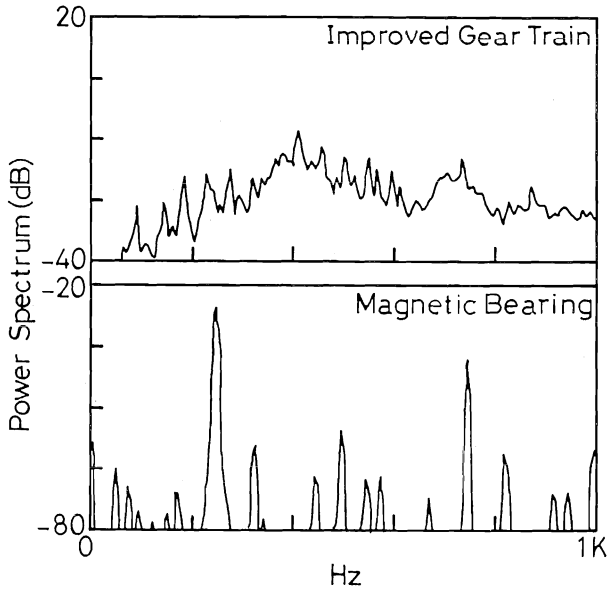

Fig.6 FFT analysis of PBREP (a)before and (b)after the installation of magnetic bearings.

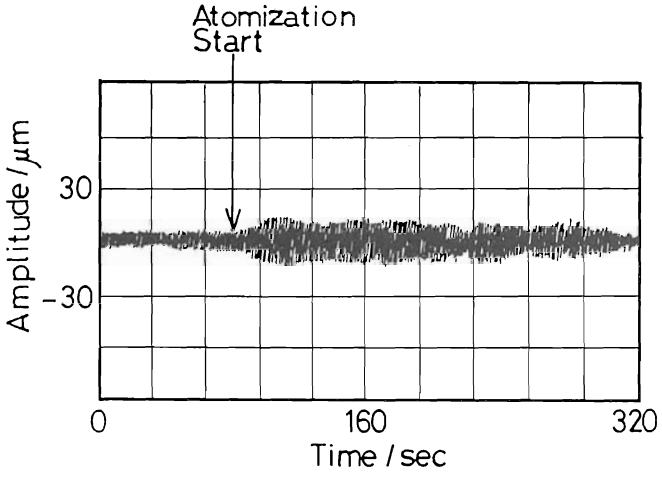

Fig.7 Change of vibration amplitude during the atomization

There are some problems remained in this system. Brush is now used at the speed of twice or more of its permissible speed. From these restriction, up to now we can not rotate the billet at its maximum speed. But improvements are in progress and it will be made possible to rotate the billet with these speeds.

4. Characteristics of Powder

Scanning Electron Microprobe (SEM) image of GT-33 Ti alloy powder produced in our PBREP equipment is shown in **Photo.3**, which shows that spherical powders were obtained. Powder made by the processes which utilize electron beam as a heat source has the surface α shell, which produced by the evaporation and deposition of alloying element such as Al with high vapor pressure. Such heterogeneity is not observed in our powder as proved by electron probe micro analysis or Auger analysis.

Particle size distribution of Ti-6Al-4V measured by micro track analysis is given in **Fig.8**. 50% line of vertical axis gives the mean diameter and its relation to rotation speed almost agrees with Eq.1,2 and **Fig.2**, but as particle diameter becomes finer, mean deviation becomes smaller.

Histogram of GT-33 powder is also given in **Fig.9**. The change of the drive system to magnetic bearings largely decreased the amount of coarse particles and resulted in a sharp distribution. The mean particle diameter became 86 μm.

Photo.4 shows the SEM image of a cross section of GT-33 powder. The microstructure is uniform in the cross section and is composed of fine cells and dendrites. The relation between the mean cell diameter and the particle size is shown in Fig.10. Each line shows the state of the drive system, and improvement of the cooling system was made together with use of 'improved gear train' and 'magnetic bearing'. It is seen that these improvement refined the substructure.

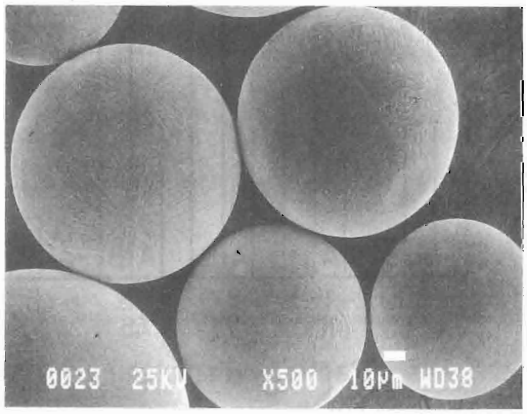

Photo.3 SEM image of GT-33 powder.

Solidification rate is estimated to be increased from $10^{2\sim3}$ at original state to $10^{4\sim5}$ °C/s after the installation of magnetic bearings.

These figures agree also with results obtained from β grain size estimation from microstructural observation of hot isostatic pressed samples and Eq.7.

Improved powder enabled HIP consolidation temperature to decrease about 100 °C. The α grain size after HIP at 750 °C was about 1μm. The flow stress of a HIP'ed preform at 850 °C and strain rate 5×10^{-4} s^{-1} was 1.7 kgf/mm^2, which is one half of that of usual powder.

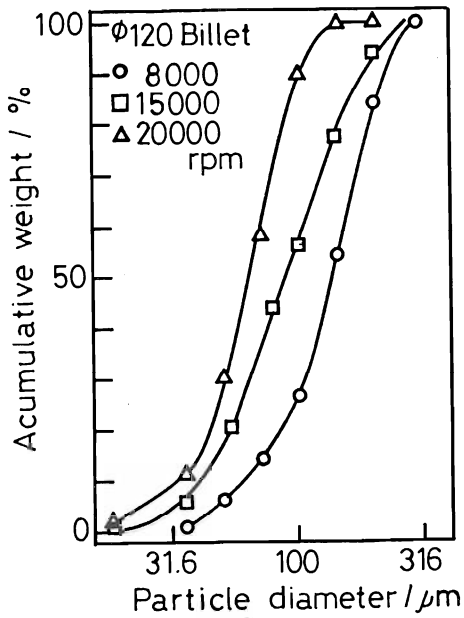

Fig.8 Particle size distribution of Ti-6Al-4V.

These preforms were successfully forged superplastically to a ϕ400mm full scale model disk with blades (blisk) under a very low forging load of 1500 tonf. After double solution heat treatment and aging, this showed ultimate strength 133.0 kgf/mm^2 (strength to density ratio 28.6 km) and elongation 11.3% at 300 °C.

Furthermore, we applied Hydride-DeHydride (HDH) process to control the microstructure of the disk. Hydrogen is a β-phase forming element and it has $10^{1\sim2}$ times larger diffusion coefficient in fine grained body. Using hydrogen as temporary alloying element, partial HDH process enabled to obtain a disk with unique microstructure (dual property disk).

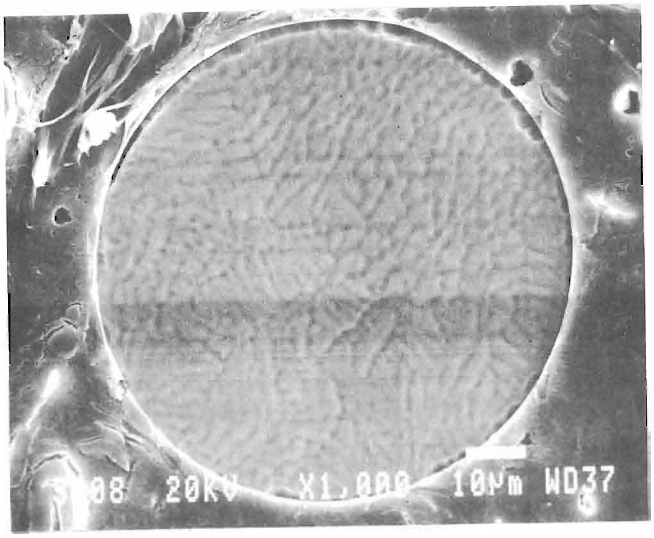

Photo.4 Cross-section of GT-33 powder.

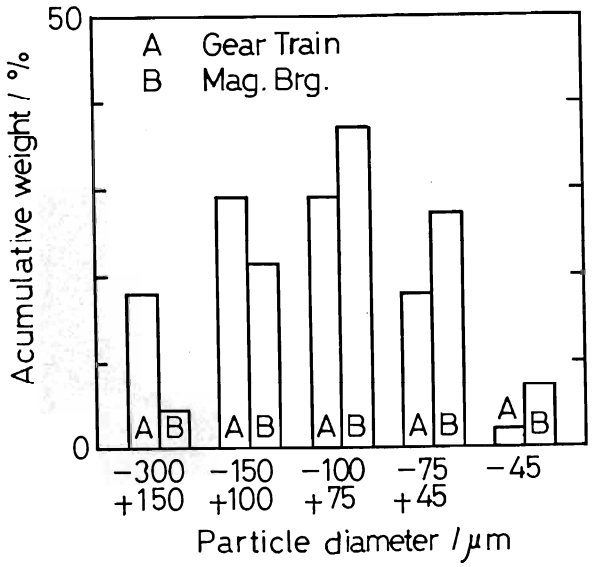

Fig.9 Particle size distributions of GT-33.

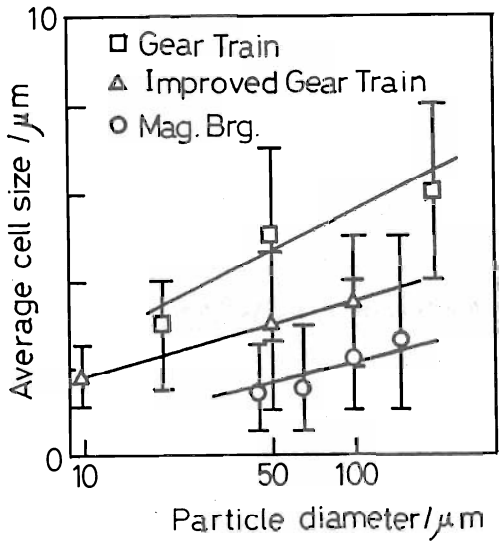

Fig.10 Relation between particle diameter and average cell size.

It consists of two portion ,and the boss part where high strength is necessary has a very fine microstructure and the blade part where creep strength is necessary possesses a coarse microstructure. The creep life of the blade portion is extended to 3 times[16].

Our equipment has not reached its maximum ability yet, but further improvement will make it possible to obtain powders which have finer than 50μm and its solidification rate is more than 10^6 ℃/s.

Powder metallurgy (P/M) of Ti alloys is thought to be promising and some case studies of aerospace parts evaluate that the cost of P/M products will be a half of that by ingot metallurgy (I/M) process. But actual applications of P/M are delayed contrary to this prediction. One of the reason of this delay may be high cost of powder because it has not been mass produced. And another reason may be that the mechanical properties of P/M parts are only equal or slightly superior to that of I/M parts and not enough to alter user's mind. The application of magnetic bearings to REP and Rotary Disk process may have possibility to solve these problems by giving higher production rate and finer and more rapidly solidified powder.

5.Conclusions

1. An application of magnetic bearings to PREP decreased drastically the vibration of machine.
2. Weight of the billet and maximum rotation number was increased due to the increase of allowable unbalance.
3. Monitoring of the shaft enabled the control of plasma to eliminate growing unbalance and resulted in stable operation.
4. These improvement enabled us to obtain powders which are finer than 100 μm and more rapidly solidified than 10^5 ℃/s.

Acknowledgements

This work was performed under management of Research and Development Institute of Metals and Composites for Future Industries as a part of the R&D project of Basic Technology for Future Industries sponsored by Agency of Industrial Science and Technology, MITI.

Reference

[1] F. H. Froes and J. E. Smugeresly (Eds.) : *Powder Metallurgy of Titanium Alloys*, AIME, 1981.
[2] N. E. Paton and C. H. Hamilton (Eds.) : *Superplastic Forming of Structural Alloys*, AIME, 1982.
[3] H. Onodera, K. Ohno, T. Yamagata and M. Yamazaki : *Proc. 6th Int. Conf. on Titanium*, France, 1988, 1191.
[4] P. R. Roberts and P. Loewenstein : Ref. 1, 21.
[5] J. H. Moll and C. F. Yolton : *Titanium Rapid Solidification Technology*, F. H. Froes and D. Eylon (Eds.), TMS-AIME, 1986, 45.
[6] D. J. Hodkin, P. W. Sutcliffe, P. G. Mardon and L. E. Russell : *Powder Met.*, 16-32(1973), 277.
[7] R. P. Fraser and P. Eisenklam : *Trans.*,Inst. Chem. Eng., London, 34(1956), 294.
[8] B. Champagne and R. Angers : *Int. J. Powder Metall. Powder Technol.*, 16-4(1980), 359.
[9] C. Acrivos : *J. Mat. Sci.*, 11(1976), 1159.
[10] S. J. Savage and F. H. Froes : *J. Metals*, 36-4(1980),20.
[11] F. H. Froes and R. G. Rowe : *Rapidly Solidified Alloys and their Mechanical and Magnetic Properties*, Materials Research Society, 58(1986), 307.
[12] Y. Nishino, T. Kimura, F. Noda and T. Yamauchi : *Progress in Powder Metallurgy*, 41(1986), 509.
[13] S. Kashu, S. Nishino and C. Hayashi : *Trans. Vac. Metall. Conf.*, 1967.
[14] H. Habermann and M. Brunet : 85-GT-221, ASME.
[15] H. Habermann and M. Brunet : 84-GT-117, ASME.
[16] T. Kimura : *Proc. 7th Symposium on Basic Technologies for Future Industries*, 1989, 111 (in Japanese).